A case study on topsoil removal and rewetting for paludiculture: effect on biogeochemistry and greenhouse gas emissions from *Typha latifolia*, *Typha angustifolia* and *Azolla filiculoides*

Merit van den Berg[1]*, Thomas Gremmen[2]*, Renske J.E. Vroom[3], Jacobus van Huissteden[1], Jim Boonman[1], Corine J.A. van Huissteden[1], Ype van der Velde[1], Alfons J.P. Smolders[2,3], Bas P. van de Riet[2]

*These authors contributed equally to this work.

[1]Department of Earth and Climate, Vrije Universiteit Amsterdam, Amsterdam, 1081 HV, Netherlands
[2]B-WARE Research Centre, Nijmegen, 6525 ED, Netherlands
[3]Department of Aquatic Ecology & Environmental Biology, Radboud University, Nijmegen, 6525 AJ, Netherlands

Correspondence to: Thomas Gremmen (t.gremmen@b-ware.eu)

Abstract. Rewetting drained peatlands for paludiculture purposes is a way to reduce peat oxidation (and thus CO_2 emissions) while at the same time it could generate an income for landowners, who need to convert their traditional farming into wetland farming. The side effect of rewetting drained peatlands is that it potentially induces high methane (CH_4) emission. Topsoil removal could reduce this emission due to the removal of easily degradable carbon and nutrients. Another way to limit CH_4 emission is the choice in paludiculture species. In this study we conducted a field experiment in the coastal area of the Netherlands, in which a former non-intensively used drained peat grassland is rewetted to complete inundation (water table ~+18 cm) after a topsoil removal of ~20 cm. Two emergent macrophytes with a high potential of internal gas transport (*Typha latifolia* and *Typha angustifolia*), and a free floating macrophyte (*Azolla filiculoides*) were introduced and intensive measurement campaigns were conducted to capture CO_2 and CH_4 fluxes, soil and surface water chemistry. Greenhouse gas fluxes were compared to a high-productive peat meadow as reference site.

Topsoil removal reduced the amount of phosphorus and iron in the soil to a large extent. The total amount of soil carbon per volume stayed more or less the same. The salinity of the soil was in general high defining the system as brackish. Despite the topsoil removal and salinity, we found very high CH_4 emission for *T. latifolia* (84.7 g CH_4 m^{-2} yr^{-1}), compared to the much lower emissions from *T. angustifolia* (36.9 g CH_4 m^{-2} yr^{-1}) and *Azolla* (22.2 g CH_4 m^{-2} yr^{-1}). The high emission can be partly explained by the large input of dissolved organic carbon into the system, but it could also be caused by plant stress factors, like salinity level and herbivory. For the total CO_2 flux (including C-export), the rewetting was effective, with a minor uptake of CO_2 for *Azolla* (-0.13 kg CO_2 m^{-2} yr^{-1}) and a larger uptake for the *Typa* species (-1.14 and -1.26 kg CO_2 m^{-2} yr^{-1} for *T. angustifolia* and *T. latifolia*, respectively) compared to the emission of 2.06 kg CO_2 m^{-2} yr^{-1} for the reference site.

Azolla and *T. angustifolia* seem to have the highest potential in reducing greenhouse gas emissions after complete rewetting of drained peatlands. When considering the total greenhouse gas balance, other factors like biomass use, and storage of topsoil after removal should be considered. Especially the latter could cause substantial carbon losses if not kept in anoxic conditions.

For *Azolla*, a follow-up study without topsoil removal would be useful, to see if the biomass production would be high while keeping CH$_4$ emissions low.

1 Introduction

35

With the increasing demand to reduce greenhouse gas (GHG) emissions to meet the climate goals, rewetting of drained peatlands has gained attention as a promising measure. Worldwide, drained peatlands are responsible for 2-5% of the total anthropogenic GHG emission and reducing these emissions therefore have potentially a large contribution in mitigating climate change (Bonn et al., 2016; Leifeld and Menichetti, 2018; Humpenöder et al., 2020). The Netherlands has 260,000 ha of drained

40 peat (6% of the total land area), mainly in use for agriculture. This area emits around 5.6 Mt CO$_2$-eq per year, which is about 3% of the total national emission (Arets et al., 2020). Besides the undesired effect of peat oxidation on the climate, it also leads to land subsidence of about 0.8 cm per year (Hoogland et al., 2012; Van den Born et al., 2016). For a country below sea level and an increasing sea level rise in prospect, this gives an extra impulse to reduce peat oxidation. By elevating the water table and thus rewetting the drained peat, anoxic conditions could be restored. Rewetting 60% of the current global degraded

45 peatlands would turn these areas into a net carbon sink by 2100 (Humpenöder et al., 2020). However, rewetting and the return of anoxic conditions lead to an increase in methane (CH$_4$) emissions and land becomes less suitable for conventional agriculture.

The increase in CH$_4$ emission after rewetting depends on the type of ecosystem and weather conditions (Abdalla et al., 2016; Hemes et al., 2018), but can be very high especially for rewetted grassland fens where availability of fresh organic matter is

50 high (Hahn-Schöfl et al., 2011; Abdalla et al., 2016; Franz et al., 2016). To minimise high CH$_4$ emissions after peat rewetting the – often nutrient-rich – topsoil can be removed prior to rewetting (Harpenslager et al., 2015; Quadra et al., 2023).

CH$_4$ has a much stronger radiative forcing than CO$_2$, making the trade-off between CO$_2$ reduction and CH$_4$ emission complex. The short lifetime of CH$_4$ in the atmosphere (compared to CO$_2$), causes the effect on global warming to be time dependent. Most commonly, a global warming potential (GWP) of 27 on a timescale of 100 years is used to estimate climate impacts of

55 CH$_4$ (IPCC, 2021). The use of this GWP can be questioned if temporal forcing dynamics are considered (Günther et al., 2020). Despite the discussion on the effect of CH$_4$ on different time scales, keeping CH$_4$ emissions as low as possible always results in the lowest impact on the climate. Vegetation type plays a crucial role in the amount of CH$_4$ that is emitted due to the species-specific influence on substrate input, oxidizing of the rhizosphere and gas transport pathways (Hahn et al., 2015; Abdalla et al., 2016; Vroom et al., 2022; Bastviken et al., 2023). Therefore, management of rewetted peatlands can be directed towards a

60 vegetation type or composition that results in the lowest CH$_4$ emission.

After rewetting, agricultural land loses its carrying capacity and conventional crops and grasses are no longer suitable to grow. A transition to (semi) natural wetland would therefore be an option, but an alternative where biomass can still be commercially used and which generates a direct income for the landowner, is paludiculture – the cultivation of wetland plants on rewetted peat. Ideally, paludiculture should result in restoration of peat accumulation (Wichtmann and Joosten, 2007). There are

65   different potentially suitable plant species for paludiculture (for a list see Abel and Kallweit, 2022). Cattail (*Typha* spp.) is a favourable option due to the high biomass production (Haldan et al., 2022) and diverse potential use as building material (De Jong et al., 2021), fodder (Pijlman et al., 2019) and biogas (Martens et al., 2021). Additionally, *Typha* has a high nutrient extraction capacity which could be helpful to improve water quality (Vroom et al., 2018). *Typha* is a genus of perennial emergent macrophytes, of which *Typha angustifolia* (narrowleaf cattail) and *Typha latifolia* (broadleaf cattail) are native to

70   Europe and common in shallow freshwater habitats such as wetlands and drainage ditches (Clements, 2022; Murphy, 2022). Their high aerenchyma content (>50% of internal leaf volume) and pressurised gas transport (Pazourek, 1977; Sebacher et al., 1985) allow them to thrive in anoxic sediments, but can also lead to high CH_4 emissions from the sediment to the atmosphere (Sebacher et al., 1985). According to previous research, *Typha* spp. may have variable effects on CH_4 emissions compared to non-vegetated conditions. Some studies indicate that they can increase CH_4 emissions (McInerney and Helton, 2016;

75   Antonijević et al., 2023), while others suggest they may lead to a decrease in CH_4 emissions (Jespersen et al., 1998; Vroom et al., 2018).

A much less discussed species in the context of paludiculture is water fern (*Azolla filiculoides*). Since its introduction from the Americas to Western Europe in the late 19th century (Pieterse et al., 1977; Sheppard et al., 2006), *Azolla* is widespread in eutrophic shallow waters such as drainage ditches. *Azolla* has several traits which potentially make it an interesting crop for

80   cultivation on rewetted agricultural lands. Because of its symbiosis with N-fixating cyanobacteria (Peters and Meeks, 1989) it has a very high potential clonal growth rate in phosphate-rich water (Wagner, 1997; Van Kempen, 2013; Li et al., 2018). Furthermore, the high protein and lipid content make it especially suitable for food and biofuel processing (Brouwer et al., 2019; Miranda et al., 2016), or biofertilizer (Bocchi and Malgioglio, 2010). Dense floating mats of *Azolla* have shown to decrease light and O_2 concentrations in the underlying surface water (Pinero-Rodríguez et al., 2021) potentially resulting in

85   increased phosphate mobilisation from the sediment to the overlying water (Boström et al., 1988).

This study was set-up to investigate the potential GHG emission reduction by three paludiculture species (from now on referred to as paludicrops): *T. latifolia, T. angustifolia,* and *A. filiculoides*, compared to high-productive drained peat grassland (from now on referred to as reference). We aim to answer the following research questions:

    1.   Can CO_2 emission reduction compensate increased CH_4 emission after peatland rewetting and introduction of the

90   three paludicrops?

        o   Which of the three paludiculture species has the highest potential in reducing GHG emissions?

    2.   What is the effect of topsoil removal and different paludicrop cultivation on soil and water nutrient concentrations?

In this study we looked at CO_2 and CH_4 dynamics in a field experiment on rewetted peat with the three different (potential) paludicrops. The experiment was conducted on a former drained and extensively managed fen grassland in West-Netherlands.

95   At this site constructed wetland basins were created and the three plant species were introduced in 2018/2019 and GHG (CO_2 and CH_4) fluxes, soil and water chemistry were monitored in 2020. The total GHG budget was compared to the reference site at 4 km distance where CO_2 fluxes were measured in the same year.

2 Materials and methods

2.1 Site description and experimental set-up

100   The experimental site was located on a former drained and non-intensively managed fen grassland in West-Netherlands (52° 43.78' N, 04° 73.15' E, Figure 1). The study started in 2018, when first ~20 cm of the topsoil was removed and used to construct embankments for the paludiculture basins. Soil properties and soil chemistry was measured before (2017) and after rewetting and topsoil removal (2018).

Our experiment was conducted in four small basins (23 x 43 m). Within this paper we included intensive greenhouse gas
105   measurements for one treatment basin (basin 2) (Figure 1C) that consisted of a water table around 20 cm above the soil surface level and no slurry or fertilizer application.
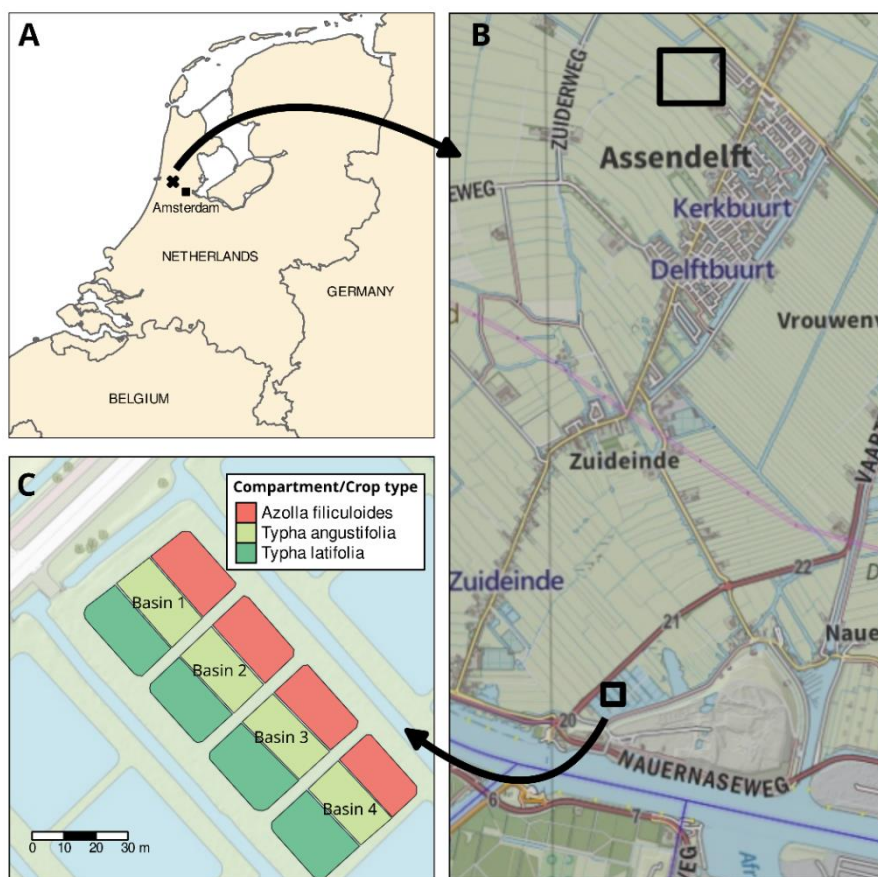
Figure 1 A) Overview of the research area located in the Netherlands (source map: SPOTinfo), with in B) the paludiculture location in the small lower square and the reference drained fen grassland in the big upper square (source map: GADM). C) Measurements
110   **for this research were conducted in Basin 2. The other basins were used to test treatments that are not discussed in this paper.**

The basins were split into three compartments (~200 m² for *Azolla*, ~430 m² for *Typha*) by vertical wooden walls. Each wall had a water inlet so water could flow passively from the inlet ditch into all three compartments. The last compartment relative to the inlet ditch contained an overflow. Together with a fixed water level in the inflow ditch, this resulted in an average water level of 18.7 (2.5 S.D.) cm above the sediment surface. Per compartment a paludicrop was planted/introduced: *Azolla filiculoides*, *Typha angustifolia* and *Typha latifolia* (Figure 1). The *Typha* species were partly planted as seedlings in autumn 2018 and partly end March 2019. *A. filiculoides* (hereafter referred to as '*Azolla*') was introduced in March 2020, by placing 950 g m⁻² fresh weight in the water. *Azolla* covered the water surface at 90-100% from May to August, after which it declined due to an infestation of the water fern weevil *Stenopelmus rufinasus*. After infestation, *Lemna* spp. gradually took over, until no Azolla was left in December 2020.

A wooden boardwalk on poles ran through the centres of each compartment to minimize disturbance during the measurements and sampling. A floating PVC frame of 3x3 m was placed to contain *Azolla* and minimize plant loss by wind. To reduce disturbance as much as possible during greenhouse gas flux measurements in the *Typha* plots, three wooden frames were installed below the water table in each *Typha* compartment (Figure 2).
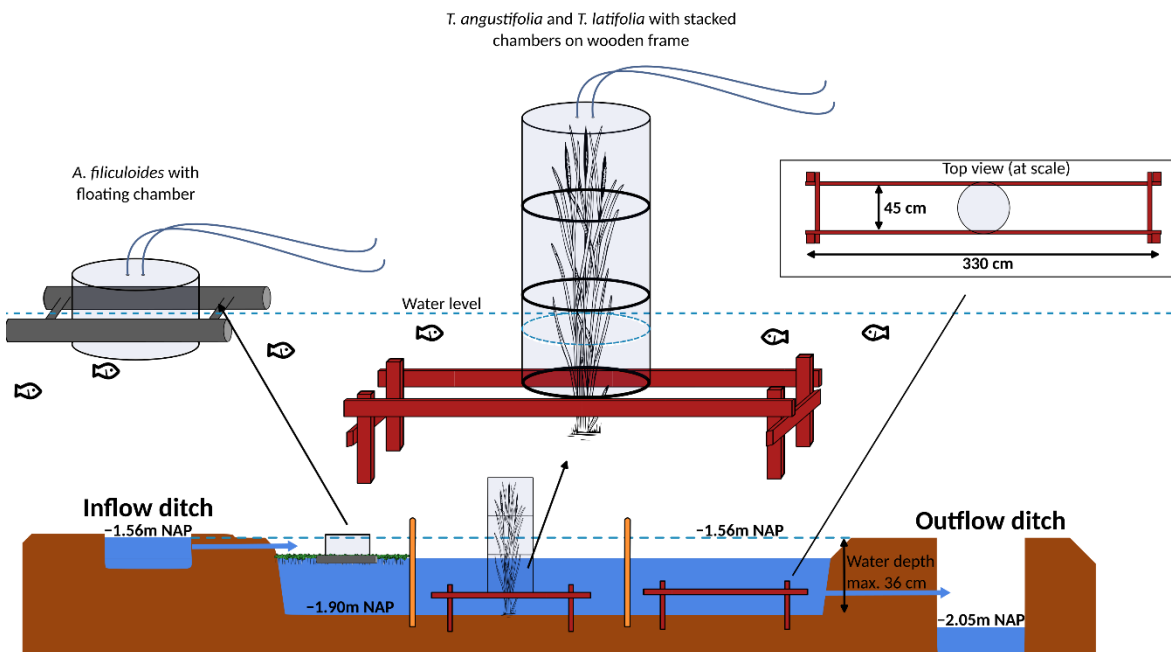
Figure 2 Set-up greenhouse gas flux measurement in experimental basin. With on the left the overview for *Azolla* and in the middle and right for *Typha angustifolia* and *Typha latifolia*, respectively. Water tables are relative to Amsterdam Ordnance Datum (NAP).

The reference site in Assendelft (N52°28'30,8", E4°44'22.7") was a managed drained peatland used for dairy farming, where perennial ryegrass (*Lolium perenne*) is grazed and harvested during the growing season. A large research plot of 24x10 m was

fenced of, in which CO_2 flux measurements were done with automated chambers and many environmental variables (like water table, soil- and air temperature, radiation) were monitored from April 2020 onwards. Chamber systems were relocated every two weeks at four different positions to minimize the effect of the chamber on temperature and vegetation growth. In 2020,

135   every four weeks from 12 May to 29 October, grass was harvested from all chamber subplots and yield was determined at the latest chamber position and from a larger reference area next to the chambers (see Boonman et al., 2022). Fertilization was done with inorganic fertilizers (250 kg N, 108 kg P_2O_5 and 195 kg K_2O ha^{-1} yr^{-1}) to prevent carbon addition to the soil. Data from the reference site were gathered in the framework of a different project and more information about the site and measurements can be found in Boonman et al. (2022).

140   **2.3 Flux measurements**

In the experimental site, CO_2 and CH_4 fluxes were measured monthly from March-December 2020 with manual chambers, and five times (March, May, July, September/October) between the manual measurements with automated chambers aiming to capture diurnal patterns.

For manual chamber measurements in both *Typha* species, transparent Perspex chambers (diameter 50 cm) were used that

145   could be stacked to match the height of the plants (Figure 3). The chambers were equipped with a fan powered by a battery. The top part additionally contained a temperature logger and PAR logger (both HOBO onset, Onset Computer Corporation, Bourne, MA, USA). For *Azolla*, a floating transparent Perspex chamber was used (diameter 29 cm, height 26 cm) equipped with a HOBO temperature logger. PAR was measured with a handheld device outside the chamber (PAR Quantum sensor SKP 215, Skye Instruments, Llandrindod, Wales, UK). Chambers were connected in a closed loop with gastight tubing to

150   either a LI-COR 7810 portable GHG analyser (LI-COR Inc, Lincoln, NE, USA) or a Los Gatos Ultra-Portable GHG analyser (ABB - Los Gatos Research, San Jose, CA, USA) that measured CO_2, H_2O and CH_4 concentrations every second. Measurements were carried out during daytime and lasted three minutes each. Fluxes were alternated between light, darkened (chambers covered with opaque white plastic film) and shaded (chambers covered with plastic shading net, reducing PAR with ~42%) measurements, to cover the PAR range as much as possible. Per measurement campaign, three light, three darkened

155   and three shaded measurements were done per species in three replicate locations (total n = 27). The increase in CO_2 and CH_4 concentrations in the chamber were visually checked for linearity in the field to ensure no ebullition occurred during the measurements. Measurements were redone if high concentration peaks, caused by ebullition, were detected. Fluxes were calculated by taking the linear fit of the concentration change in the first 1-3 minutes after closing the chamber.

Automated chambers consisted of four Perspex chambers with a diameter 35 cm and a height of 50 cm. The chambers can be

160   extended up to 150 cm in height to match vegetation height (Figure 1) and were placed in one vegetation type at the time, measuring three days per vegetation type. These chambers were equipped with fans and DS18b50 temperature sensors. Furthermore, they had hinged lids controlled by a connected Raspberry Pi computer (Raspberry Pi Foundation, Cambridge, UK) and were connected with gastight tubing in three closed loops to a Los Gatos Microportable Greenhouse Gas Analyzer (ABB - Los Gatos Research, San Jose, CA, USA). The four chambers were measured in succession, by closing the lid of a

165 respective chamber for 2.5 minutes, followed by one minute of flushing the chamber and gas analyser with atmospheric air, and then closing the lid of the next chamber, measuring, and flushing. This sequence continued for three days in each vegetation type, providing high resolution data including diurnal variation in emissions.

Figure 3 Automated chamber (left), manual chamber (middle), and bubble trap (right), used for measuring fluxes.

170

From March till December, ebullitive CH_4 fluxes were captured with bubble traps from the three paludicrops. Three bubble traps were installed in each vegetation type (total n = 9). These traps consisted of a small floating foam raft with inserted a funnel (diameter 20 cm) on the bottom part connected to a glass tube above the raft (Figure 3). To prevent ducks from sitting on the raft, toothpicks were inserted in the foam. A butyl stopper was fitted at the top of each glass tube to enable gas extraction.

175 Gas volume was determined every 1.5-3 weeks by removing the captured gas with a syringe. To determine CH_4 concentrations, gas was sampled once (April, May, November, December) or twice (June – October) a month. CH_4 concentrations of 1 ml of diluted gas sample was measured with a Los Gatos Ultraportable GHG analyser using an open loop of gastight tubing. As the CH_4 concentrations in the sampled gas were more than a factor 10000 higher than atmospheric CH_4 concentrations in the bottles and the greenhouse gas analyser, inflow was negligible.

180 CO_2 fluxes in the reference site (Assendelft) were measured with four automated chambers, connected in a closed loop to a LI-850 CO_2 gas analyzer (LI-COR, USA). The chambers had a height of 0.5 m and a diameter of 0.4 m. Every 15 minutes, each chamber measured for 3 minutes. More details about this chamber set-up and measurements can be found in Boonman et al. (2022).

2.4 Partitioning and interpolation of fluxes

185 Measured net ecosystem exchange for CO_2 (NEE) from manual chambers and automated chambers averaged over 30 minutes were partitioned into gross primary production (GPP) and ecosystem respiration (R_{eco}) so that the Lloyd-Taylor function (Lloyd & Taylor, 1994, (1)) and the light response curve could be fitted. The obtained parameters were used for interpolation of GPP and R_{eco} between the measurement campaigns. The Lloyd-Taylor function was defined as:

$$R_{eco} = R_{ref} \times e^{E_0 \times \left(\frac{1}{T_{ref} - T_0} - \frac{1}{T - T_0} \right)} \tag{1}$$

190

where R_{ref} = respiration at reference temperature (T_{ref}); E_0 = long term ecosystem sensitivity coefficient; T_0 = base temperature between 0 and T (227.13 K, Lloyd & Taylor, 1994); T = observed temperature (K); T_{ref} = reference temperature (K).

E_0 was determined by fitting E_0 and R_{ref} using the entire dataset, were T_{ref} of 283.15 K was used, T was represented by average soil temperature at 5 cm depth, and the observed R_{eco} were averaged dark or night-time CO_2 fluxes per measurement

195 campaign/day. With the gained E_0, R_{ref} per measurement campaign/day at a T_{ref} of 283.15 K was determined by inverse the Lloyd-Taylor function with the average measured dark or night-time CO_2 flux as R_{eco}, and the average soil temperature at 5 cm depth as T. R_{ref} was linearly interpolated between the measurement campaigns. Both R_{ref} and E_0 were used to calculate R_{eco} for every 30 minutes with measured soil temperature when data was absent.

Daytime fluxes were partitioned based on the standard procedure as used in e.g. Falge et al. (2001), Veenendaal et al. (2007)

200 and Tiemeyer et al. (2016). GPP was gained from the NEE, by subtracting calculated R_{eco}: GPP = NEE – R_{eco}. The parameters α and GPP_{max} of a hyperbolic light response equation based on the Michaelis–Menten kinetic (2), were fitted on the given GPP.

$$GPP = \frac{(\alpha \cdot PAR \cdot GPP_{max})}{(\alpha \cdot PAR + GPP_{max})} \tag{2}$$

where α is the initial slope of the light response curve; GPP_{max} is the light-saturated photosynthetic rate and PAR is the

205 measured photosynthetically active radiation. GPP_{max} and α were linearly interpolated between the measurement campaigns and used to calculate GPP on 30-minute base when no data were present.

CO_2 partitioning and gap filling (interpolation) was slightly different for the automated chambers on the reference location Assendelft, since the data density was much higher and R_{eco} was determined from night-time data and calculated for daytime based on the temperature response of the Lloyd-Taylor relation. For more details see (Boonman et al., 2022). The only

210 difference is the missing data from January 2020-March 2020, since measurements started in April 2020. R_{eco} for this period was estimated by fitting the Lloyd-Taylor function on the winter period January-March for the years 2021-2023 and using the gained R_{ref} and E_0 with the measured soil temperature in that period. To estimate GPP in 2020, we used the monthly average

of the parameter α and the GPP$_{max}$ for January – March for 2021, since first harvest of 2020 and 2021 were similar, together with measured PAR.

215 For CH$_4$, there is no standard interpolation procedure, and part of this study was therefore to find to best relation between environmental variables and diffusive fluxes. It appeared that soil temperature correlated highest with CH$_4$ fluxes from *Typha*, and water temperature with fluxes from *Azolla* with an exponential relation (see section 3.3 Methane fluxes).

2.5 Vegetation measurements

To estimate the biomass of *Typha* spp. in the measurement plots, ten living shoots were harvested for each species outside of
220 the measurement plots in September 2020. These shoots were dried at 70 °C for 72 hours, and dry weight per cm biomass was calculated. This was then multiplied by the number of living shoots and the average shoot height at each measurement time and in each subplot to estimate the biomass at each measurement day. For the C-export term, the average amount of dead stems was subtracted from the amount of living stems from the measurement plots, and with the above-described relation used to determine the extra amount of biomass produced in 2020. This was called C-export since this could have been the potential
225 net term of carbon loss by harvest.

2.6 Sample collection

Soil samples of the original drained grass meadow before topsoil removal and rewetting were collected in March 2017. Samples were collected at five locations, divided over the area where the four experimental paludiculture basins were planned, at a depth of 0-10, 10-20 and 20-30 cm below surface level. After topsoil removal and rewetting, additional samples were collected
230 in November 2018 in the four experimental basins. Here, five samples of the inundated topsoil (0-10 cm) were collected in each compartment of the four basins, after which the samples were pooled per compartment before analysis. All samples were stored in airtight plastic bags at 4 °C until further analysis.

Surface water and pore water samples were collected monthly directly after manual chamber measurements in the experimental basins and inflow- and outflow ditches. Surface water samples were taken by hand in the inlet water ditch and each
235 compartment (n=1 per compartment/ditch). Pore water was collected anaerobically with a 60 ml syringe attached to a ceramic cup via gas-tight tubing, which was installed in the top 15 cm of the sediment in each respective compartment. Additional pore water samples for dissolved CH$_4$ and sulphide (H$_2$S) were collected by attaching a gas-tight pre-vacuumed 12 ml glass exetainer (containing 1 ml of 0.5M HCl to stop microbial activity; Labco, Lampeter, UK) via a hypodermic needle to the gas-tight tubing. The exetainers were stored upside down to minimise the risk of gas leakage. All samples were stored at 4 °C until
240 further analysis.

2.7 Soil analysis

Two aluminium cups (40.5 mL) were filled with fresh soil and weighed before and after drying at 60 °C for >48 hrs to obtain the wet weight and bulk density, respectively. Thereafter, one cup with dried soil was incinerated (4 hrs at 550 °C) and weighed

again to determine organic matter (as loss on ignition). Total phosphorus (P), iron (Fe) and sulphur (S) content were determined
245 by digesting 200 mg of homogenised finely ground soil with 5 ml 65% HNO_3 and 2 ml H_2O_2 in a microwave (Ethos Easy,
Milestone, Sorisole, Italy). Samples were then diluted to 100 ml with demineralised water and analysed using inductively
coupled spectrometry axial plasma observation, seaspray nebulizer, 1300 W, 12 l min^{-1} (ICP-OES ARCOS MV, Spectro
Analytical Instruments, Kleve, Germany). Plant-available extractable inorganic nitrogen was determined by incubating 17.5 g
of fresh soil with 50 ml of 0.2M NaCl for 2 hrs with 105 rpm and at room temperature. After determining the pH (PHC101
250 probe connected to HQ440d, Hach, Düsseldorf, Germany), the extract was collected using soil moisture samplers (Rhizon
SMS, Eijkelkamp, Giesbeek, Netherlands), and analysed colourimetrically for nitrate (NO_3^-) and ammonium (NH_4^+) on a Seal
auto-analyser III using hydrazine sulphate and salicylate reagent, respectively. Plant-available extractable phosphorus (Olsen-
P) was determined by incubating 3 g of dried homogenised finely ground soil with 60 ml 0.5 M $NaHCO_3$ at pH 8.5 for 30 min
with 105 rpm and at room temperature. The pH of the medium was adjusted before incubation by adding NaOH when
255 necessary. The extracted medium was diluted ten times with demineralised water and stored at 4°C until further analysis on
ICP-OES as described above.

2.8 Surface water and pore water analysis

The pH was measured using a standard Ag/AgCl2 electrode connected to a Radiometer (Copenhagen, Type TIM840). The
total inorganic carbon (TIC) concentration was determined by injecting a known amount of sample into an infra-red gas
260 analyser (ABB Advance Optima IRGA), after which the concentrations of CO_2 and HCO_3^- were calculated based on the pH
equilibrium. Concentrations of nitrate (NO_3^-) and ammonium (NH_4^+) were determined colourimetrically on an auto-analyser
as described above. Chloride (Cl^-) and phosphate (PO_4^{3-}) concentrations were determined colourimetrically on a Bran+Luebbe
auto-analyser III system using respectively mercury(II)cyanide and ammonium molybdate/ascorbic acid as the reagent.
Acidified samples (0.1 ml 65% HNO_3) were analysed for total-Fe, total-P and total-S on ICP-OES as described above. After
265 equilibrating to atmospheric pressure with N_2 gas, the concentrations of methane (CH_4) and sulphide (S^{2-}) were measured in
the headspace of the exetainers by injecting into a 7890B gas chromatograph (Agilent Technologies, Santa Clara, USA)
equipped with a Carbopack BHT100 glass column (2 m, ID 2 mm), flame ionization (FID) and flame photometric detector
(FPD. Concentrations of dissolved organic carbon (DOC) were measured on a TOC-L CPH/CPN analyser (Shimadzu) after
acidification with HCl to remove DIC.

270 ## 2.9 Environmental variables

Surface water and groundwater levels were calculated based on hourly measurements of atmospheric pressure (Baro-Diver,
Eijkelkamp, Giesbeek, Netherlands) and water pressure at a known depth (Cera-Diver, Eijkelkamp, Giesbeek, Netherlands).
Air temperature was also measured hourly (Baro-Diver, Eijkelkamp, Giesbeek, Netherlands). Soil and water temperature was
monitored with a 2-minute interval in all four basins (HOBO S-TMB temperature probe connected to H21-USB station, Onset,
275 Bourne, MA, USA). Water temperature was measured in the *T. angustifolia* compartment of each basin, and soil temperature

was measured at 5 cm depth in each compartment. Photosynthetic active radiation (PAR) was monitored with a 2 min interval at 3 m above water level using a HOBO S-LIA-M003 PAR sensor connected to a H21-USB station (Onset, Bourne, MA, USA).

3. Results

280 **3.1 Environmental conditions**

The study was conducted in the year 2020, which was a slightly warmer (+0.9 °C) year than the 10-year average 2001-2020 (Royal Netherlands Meteorological Institute KNMI). The yearly average precipitation was very similar to average (862 mm in 2020) but the summer period (Jun-Sep) was dryer (337 mm vs 474 mm).

The seasonal dynamics are clearly visible in all variables. The groundwater table of the reference site reaches a minimum of -285 86 cm in August (Figure 4). The water table in the paludiculture basin was kept more or less constant at +18 cm. Due to this water layer, the soil temperature fluctuations in the paludiculture basin were much more dampened than within the reference site (Figure 4).
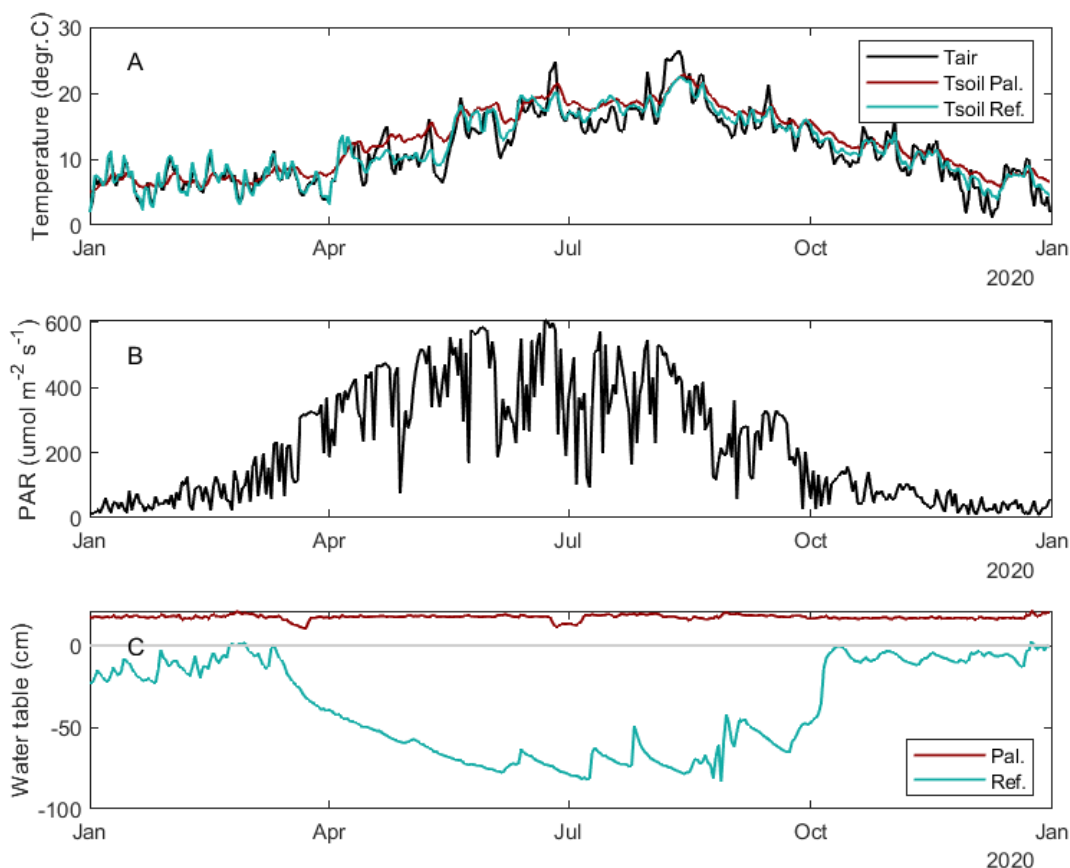
Figure 4 (A) Air temperature (Tair) and site-specific soil temperature (Tsoil) for paludiculture site (Pal.) and reference site (Ref.),
290   **(B) photosynthetically active radiation (PAR), and (C) (ground)water table for the paludiculture site (Pal.) and reference site (Ref.).**

3.2 Effect of rewetting and plant growth on surface and pore water chemistry

After topsoil removal, the total amount of organic matter remained the same in the upper soil layer, but bulk density in the top layer (0-10 cm) was reduced by about 50% (Table 1). Also, total phosphorus and total iron decreased quite drastically by about
295   65%, whereas total sulphur increased with 81%, which could lead to an increase in (toxic) free sulphide in the rootzone (Table 1). Assuming 58% of OM was carbon (C) (van Bemmelen factor), the removal of ~20 cm of the topsoil resulted in the displacement of approximately 15.8 kg C m^{-2}.

300 **Table 1 Soil properties of bulk density (BD), organic matter content (OM), total phosphorus (Total-P), plant-available phosphorus (Olsen-P), total iron (Total-Fe), and total sulphur (Total-S) before rewetting (RW) in 2017 (n=5), and after rewetting and topsoil removal in 2018 (n=12). Because ~20 cm of topsoil is removed, the depth 0-10 cm after RW correspond to the soil layer 20-30 cm of before RW. Numbers within brackets denote the standard deviation.**

Parameter	Unit	Before RW			After RW
		0-10 cm	10-20 cm	20-30 cm	0-10 cm
BD	kg dw l^{-1}	0.44 (0.14)	0.35 (0.19	0.20 (0.06)	0.24 (0.06)
OM	%	34 (13)	50 (27)	70 (19)	61 (13)
OM	g dw l^{-1}	135 (18)	138 (23)	132 (14)	138 (11)
Total-P	mmol l^{-1}	15 (3.4)	7.1 (3.2)	3.2 (1.5)	5.3 (2.0)
Olsen-P	mmol l^{-1}	0.98 (0.15)	0.51 (0.22)	0.18 (0.11)	0.30 (0.13)
Total-Fe	mmol l^{-1}	173 (73)	167 (117)	53 (29)	61 (27)
Total-S	mmol l^{-1}	48 (15)	61 (18)	73 (13)	87 (14)

305

Surface water and pore water chemistry was measured during the whole measurement period in 2020 (Figure 5 and Figure 6). Surface water ammonium (NH_4^+) and nitrate (NO_3^-) concentrations were relatively low throughout the growing season (< 25 µmol l^{-1} and < 8 µmol l^{-1}, respectively). The concentration of phosphate (PO_4^{3-}) was also low throughout the growing season in both *Typha* compartments (< 2.5 µmol l^{-1}) but increased in the inlet water ditch to 9.2 µmol l^{-1} in July. The pH varied

310 between 7 and 8.6, with the highest values in the period May-September and the lowest in winter (Table A1, Appendix). The Chloride (Cl^-) concentration also showed a clear seasonal pattern, with relatively low concentrations in winter (~20 mmol l^{-1} in February) and high concentrations in summer (~60 mmol l^{-1} in August 2020). Total sulphur (TS) was highly variable over time but was generally lower in both *Typha* compartments (221-887 µmol l^{-1} in *T. Angustifolia* and 127-432 µmol l^{-1} in *T. latifolia*), compared to the *Azolla* compartment (387-1291 µmol l^{-1}) and the water inlet ditch (495-1414 µmol l^{-1}).

315 In the pore water, NH_4^+ and total phosphorus (TP) concentrations were low throughout the year in both *Typha* compartments (< 30 µmol l^{-1} and < 4.4 µmol l^{-1}, respectively). In the *Azolla* compartment, however, NH_4^+ was substantially higher with concentrations ranging from 130 µmol l^{-1} in July 2020, to 650 µmol l^{-1} in September 2020. TP increased from 10 µmol l^{-1} in March to 50 µmol l^{-1} in October. The Cl^- concentration in the pore water showed a seasonal pattern as well, with 20-40 mmol l^{-1} in March 2020 to 45-70 mmol l^{-1} in October 2020. In the *Azolla* compartment, pore water was very iron (TFe) and sulphur

320 (TS)-rich in March and April 2020 (> 3000 and > 1000 µmol l^{-1}, respectively, Table A2, Appendix), but dropped to concentrations similar to both *Typha* compartments during the summer. Sulphide (S^{2-}) concentrations in the pore water were very low (< 0.2 µmol l^{-1}) throughout the year in all three compartments (Table A2, Appendix).
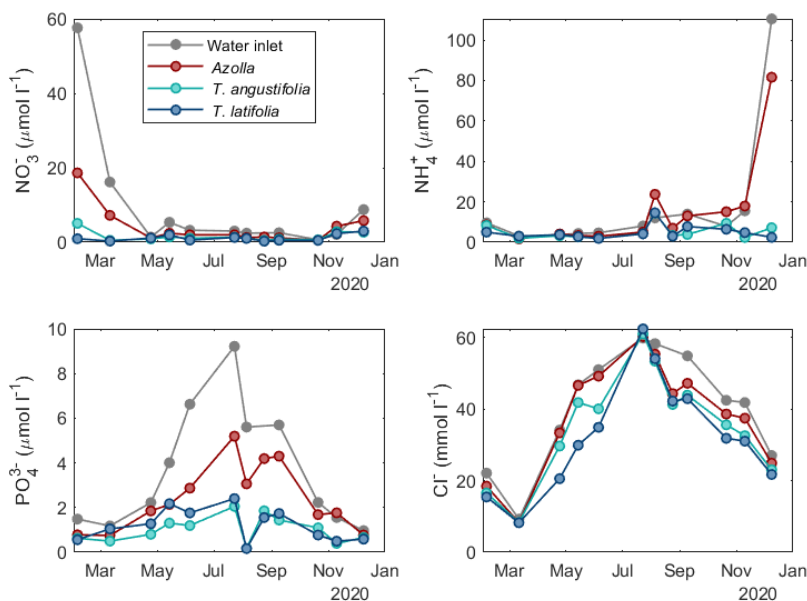
Figure 5 Surface water chemistry of nitrate (NO$_3^-$), ammonium (NH$_4^+$), phosphate (PO$_4^{3-}$), and chloride (Cl$^-$) measured in the different compartments of the three paludicrops, and in the water inlet ditch at different moments in time.
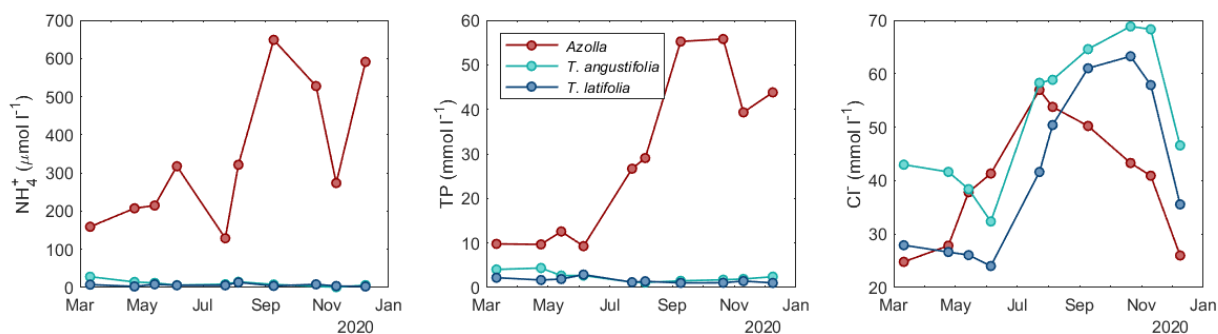
Figure 6 Pore water chemistry of ammonium (NH$_4^+$), total phosphorus (TP), and chloride (Cl$^-$) measured in the soil of the different compartments of the three paludicrops at different moments in time.

3.3 Methane fluxes

Diffusive CH$_4$ fluxes were measured with chambers and ebullition with bubble traps for all three paludicrops, but not on the reference site since that was not inundated. For interpolating CH$_4$ fluxes to come to a year budget, relations with environmental variables were analysed for the three vegetation types. Diffusive CH$_4$ fluxes from *T. latifolia* and *T. angustifolia* showed the strongest correlation with living above ground biomass (R^2 = 0.78 and 0.63, respectively). However, this variable is not useful for interpolation, since we do not have biomass data between the measurement campaigns. Soil temperature was the second-best explanatory factor for CH$_4$ emission for both *Typha* species (R^2 = 0.63 for *T. latifolia*; R^2 = 0.58 for *T. angustifolia*), and

had a very strong correlation with aboveground biomass ($R^2 = 0.94$ for *T. latifolia*; $R^2 = 0.95$ for *T. angustifolia*). For *Azolla*, water temperature correlated slightly better ($R^2 = 0.45$) than soil temperature ($R^2 = 0.37$). Therefore, for *Typha*, we used soil
340   temperature and for *Azolla* water temperature for interpolating the diffusive CH_4 fluxes (Figure 7).
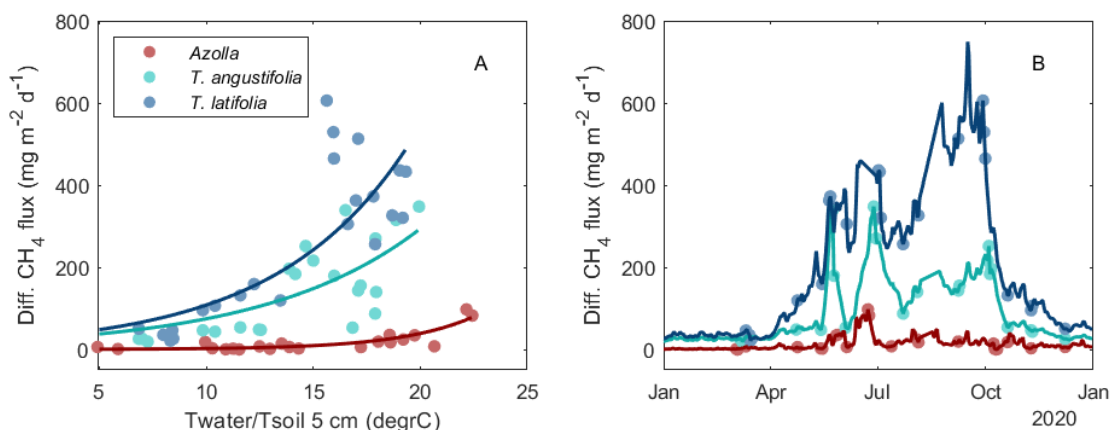
Figure 7 Relation between daily mean diffusive CH_4 flux with water temperature (*Azolla*) or soil temperature at 5 cm depth (*Typha angustifolia*, *Typha latifolia*) (A). And measured and interpolated (lines) diffusive CH_4 flux by using the temperature relation (B).

345   Ebullition measurements were considered as the average ebullitive flux over the period the ebullition traps were in the field. So, no interpolation was needed, but fluxes were summed. However, for January-February there were no measurements yet, and data from March was used.

The yearly sum of CH_4 flux was highest for *T. latifolia* and lowest for *Azolla*, with the highest absolute and relative contribution of ebullition for *Azolla* (Table 2).

350

Table 2 Total CH_4 flux for 2020 for *T. angustifolia*, *T. latifolia* and *Azolla*. Total flux consists of diffusive flux and ebullition flux. The number between brackets denotes the standard deviation, representing the variation between the measurement replicates. For the calculation of CH_4 fluxes in CO_2 equivalent (CO_2-eq), a GWP_{100} of 27.2 is used (IPCC, 2021).

Species	CH_4 diffusion (g CH_4 m^{-2} yr^{-1})	CH_4 ebullition (g CH_4 m^{-2} yr^{-1})	Total CH_4 flux (g CH_4 m^{-2} yr^{-1})	Total in CO_2-eq (t CO_2-eq ha^{-1} yr^{-1})	% ebullition (%)
T. angustifolia	33.6 (19.2)	3.2 (5.2)	36.9 (20.0)	10.0	9
T. latifolia	76.2 (42.7)	8.5 (12.2)	84.8 (49.3)	23.1	10
Azolla	5.1 (5.9)	17.2 (24.2)	22.3 (25.9)	6.1	77

355   **3.4 Carbon dioxide fluxes**

CO_2 fluxes always reflect a combination of different processes: daytime uptake of CO_2 by plant photosynthesis (GPP), and ecosystem respiration (R_{eco}) as the sum of plant respiration for maintenance and growth (autotrophic respiration) and soil

respiration (heterotrophic respiration). R_{eco} showed large differences between the different paludicrops and over the seasons (**Figure 8**). For the three different species, the total year sum of CO_2 was the highest for *T. latifolia*, but R_{eco} was still around half of that from the reference site (Table 3 Yearly interpolated CO_2 fluxes, consisting of ecosystem respiration (R_{eco}), gross primary production (GPP), net ecosystem exchange (NEE), carbon removed from harvest (C-export), and the sum of NEE and C-export (Total CO_2)). *T. latifolia* had a higher GPP compared to *T. angustifolia*, but this could only partly explain the difference in R_{eco}. *Azolla* clearly had the lowest GPP (and thus biomass production) and the lowest R_{eco}. However, in relation to the GPP, R_{eco} was relatively high, resulting in the highest NEE (Table 3).
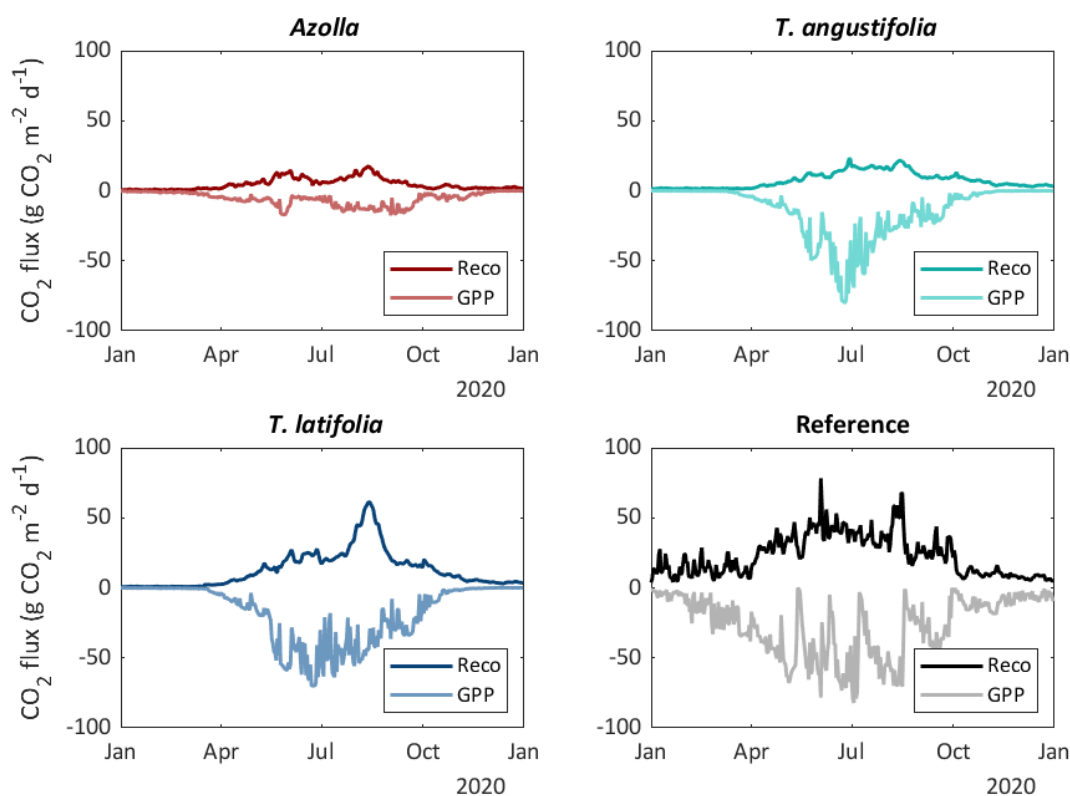
Figure 8 Estimated daily average ecosystem respiration (R_{eco}) and gross primary production (GPP) for the three paludicrops and the drained reference site.

To derive an annual CO_2 balance, the fluxes were interpolated (see methods Sect. 2.4) over the entire year (**Figure 8**). Harvested biomass, converted to CO_2 (C-export), was added to come to the complete CO_2 balance. The harvested biomass was corrected for the biomass that was left in the previous year (not harvested), to avoid double counting. In total, we observed that the net uptake of CO_2 was greater than the yield, meaning that the CO_2 balance results in a CO_2 uptake of the system for all crops, with the highest uptake (-1.26 kg CO_2 m^{-2} yr^{-1}) for *T. latifolia* and lowest uptake for *Azolla* (-0.13 kg CO_2 m^{-2} yr^{-1}) (Table 3).

Table 3 Yearly interpolated CO_2 fluxes, consisting of ecosystem respiration (R_{eco}), gross primary production (GPP), net ecosystem exchange (NEE), carbon removed from harvest (C-export), and the sum of NEE and C-export (Total CO_2). The number between brackets denotes the standard deviation, representing the variation between the measurement replicates. For *Typha* C-export two samples were taken, so no standard deviation could be determined.

Species	R_{eco} $kg\ CO_2\ m^{-2}\ yr^{-1}$	GPP $kg\ CO_2\ m^{-2}\ yr^{-1}$	NEE $kg\ CO_2\ m^{-2}\ yr^{-1}$	C-export $kg\ CO_2\ m^{-2}\ yr^{-1}$	Total CO_2 $kg\ CO_2\ m^{-2}\ yr^{-1}$
T. angusifolia	2.78	-5.15	-2.37 (1.9)	1.23 (0.89)	-1.14 (2.1)
T. latifolia	4.72	-6.45	-1.72 (1.5)	0.46 (0.15)	-1.26 (1.6)
Azolla	1.73	-2.04	-0.31 (0.43)	-	-0.13 (0.43)
Reference	8.38	-9.79	-1.41 (0.12)	3.47 (0.39)	2.06 (0.41)

3.5 Total greenhouse gas balance

When considering both CO_2 and CH_4 emissions in CO_2-equivalents (CO_2-eq), only *T. angustifolia* had a higher uptake of CO_2 (also considering C-export) than the CH_4 that was emitted, making it a net GHG sink (-1.4 t CO_2-eq. $ha^{-1}\ yr^{-1}$). With the other two species, CH_4 in CO_2-eq emission was higher than CO_2 uptake, with a higher emission for *T. latifolia* (10.5 t CO_2-eq. ha^{-1} yr^{-1}) than for *Azolla* (2.9 t CO_2-eq $ha^{-1}\ yr^{-1}$) (Figure 9). However, all paludicrops had a lower net emission than the reference site (20.6 t CO_2-eq $ha^{-1}\ yr^{-1}$).
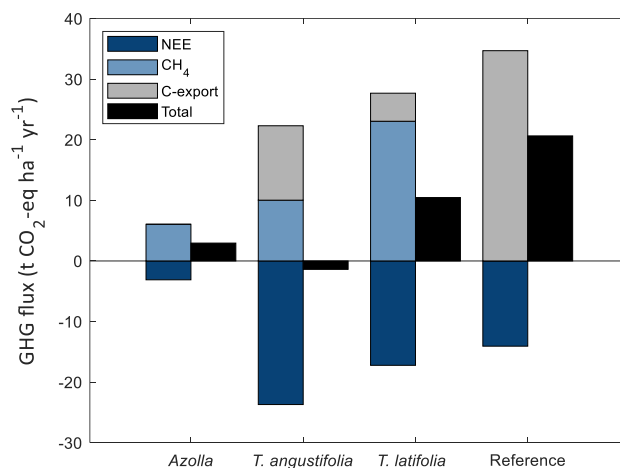
Figure 9 Greenhouse gas (GHG) balance for the three paludicrops and the reference site. GHG balance consists of net ecosystem exchange of CO_2 (NEE), carbon removed by harvest (C-export) and CH_4 flux (consisting of ebullition and diffusive fluxes) expressed in CO_2 equivalent (GWP_{100} of 27.2, IPCC, 2021), and the total net flux as the sum of the three terms. *Typha* yield was corrected for the biomass that was left in 2019. Therefore, it does not represent the potential yield from the *Typha* fields.

4. Discussion

4.1 Differences in CH$_4$ flux of the three paludicrops

We found large differences in diffusive and ebullitive CH$_4$ fluxes from the three investigated plant species. The differences in

395 CH$_4$ fluxes, with lowest diffusive and highest ebullitive fluxes for *Azolla*, can be well explained by the differences in growth forms and species-specific characteristics. A more thorough discussion of the effects of these plants on CH$_4$ emissions can be found in Vroom et al. (in prep.). Briefly, *Azolla,* a free-floating plant without roots in the soil, neither releases root exudates to the sediment, nor transports sediment CH$_4$ to the atmosphere. Moreover, radial oxygen loss (ROL) from roots can lead to oxidation of up to 70% of the produced CH$_4$ (Kosten et al., 2016). This may explain the relatively low CH$_4$ diffusion from

400 Azolla, which has been found for other free-floating species before (Attermeyer et al., 2016). On the other hand, CH$_4$ emissions by ebullition are still substantial, probably due to the release of dead roots and root exudates to the water, providing carbon for methane production. In the case of *Typha*, plant mediated transport is substantial (Bendix et al., 1994; Yavitt and Knapp, 1998; White and Ganf, 2000) and CH$_4$ production in the sediment can be increased by the supply of carbon through the roots. The plant transport of CH$_4$ causes the CH$_4$ concentration in the soil to decrease, which leads to a lower ebullition flux (Van der Nat

405 et al., 1998; Grünfeld and Brix, 1999; Van den Berg et al., 2020). So, although rates of methane production may be higher due to the supply of easily degradable carbon, which will increase over the course of the season as the plants grow larger (Joabsson and Christensen, 2001), the build-up of CH$_4$ in the sediment will remain low. Lower emissions from *T. angustifolia* than *T. latifolia*may be explained by the greater ability of *T. angustifolia* is able to build up pressure in the stem and higher ROL rates compared to *T. latifolia* (Bendix et al., 1994; Matsui Inoue and Tsuchiya, 2008), resulting in higher rates of methane

410 oxidation(Bendix et al., 1994). Additionally, in 2020, 90% of *T. latifolia* had been damaged by the webb's wainscot and/or the bulrush wainscot, which may have reduced pressurized flow (Armstrong et al., 1996). The total CH$_4$ emission in 2020 for *T. latifolia* was high, both relative to the other species and in absolute terms (84.8 g CH$_4$ m^{-2} yr^{-1}). Emissions were around a factor ~1.7 higher than what was found in a similar experiment in the Netherlands (Buzacott et al., In prep.), but the same magnitude was found in a boreal lake in Canada (Desrosiers et al., 2022). However, Rey-Sanchez et al. (2018) show even higher emissions

415 from a natural system in the USA than what we found (292 g CH$_4$ m^{-2} yr^{-1}). They hypothesize that the high fluxes could be attributed to high DOC input. This could also be the case in our site, as high DOC values (5.3 mmol l^{-1}, Table A1) were found in the inflow ditch water. Another reason could be plant stress factors, like salinity level and herbivory, resulting in enhanced die-off of plant material. Both could lead to higher substrate availability for CH$_4$ production. *T. angustifolia* was less affected by herbivory and has a higher salt tolerance than *T. latifolia* (McMillan, 1959).

420 The lower CH$_4$ emission for *T. angustifolia* compared to other rooting wetland plants was also found in another study, where fluxes from *Phalaris* and *Phragmites* were a factor 1.7 and a factor 2 higher, respectively (Maltais-Landry et al., 2009). Absolute CH$_4$ emissions from *T. angustifolia* vary strongly from ~11 g CH$_4$ m^{-2} yr^{-1} in a constructed wetland (Maltais-Landry et al., 2009), to ~176 g CH$_4$ m^{-2} yr^{-1} in a natural wetland in Canada (Strachan et al., 2015), compared to our 36.9 g CH$_4$ m^{-2} yr^{-1}. But not many studies were found.

425 For *Azolla*, all studies on CH_4 fluxes we found were conducted in combination with rice growth. These studies show in general a decrease in CH_4 emission with the addition of *Azolla* to rice paddies (Bharati et al., 2000; Liu et al., 2017; Xu et al., 2017; Kimani et al., 2018). This is in line with our observations, where we found a factor 1.7-3.8 lower emissions from *Azolla* compared to *Typha*.

Overall, our measured CH_4 fluxes were high despite the topsoil removal and the brackish conditions, which were expected to
430 reduce CH_4 production, due to the removal of easily degradable carbon (Harpenslager et al., 2015; Quadra et al., 2023) and the reducing effect of salinity on CH_4 production (Van der Gon and Neue, 1995; Minick et al., 2019), respectively.

4.2 CO_2 reduction and biomass use

Paludiculture reduced the net CO_2 balance (including C-export) to a large extent compared to the reference site, going from a net source (+20 t CO_2 ha^{-1} yr^{-1}) to a net sink (-1.3 t CO_2 ha^{-1} yr^{-1} *Azolla*; -11.4 t CO_2 ha^{-1} yr^{-1} *T. angustifolia*; and -12.6 t CO_2
435 ha^{-1} yr^{-1} *T. latifolia*). This shows that the rewetting was effective to stop peat oxidation. It is questionable to what extend the carbon storage measured in the *Typha* species will continue in the future. As the species were introduced in the years before (2018-2019), it is most likely there is still biomass build-up, like rhizomes, which will come to a steady state and reduces the net uptake. In literature, lower uptake values for *Typha* were found, like the range of NEE of -4 to +5 t CO_2 ha^{-1} yr^{-1} from a rewetted fen in Belarus (Minke et al., 2016). With *Azolla* the biomass completely disappeared by the end of the measurement
440 year (die-off due to herbivory), and the net CO_2 emission was close to zero. From the growth rate observed at the same field site one year later the expected biomass in a growing season could potentially reach 23-35 t dm ha^{-1} yr^{-1} (Gremmen et al., 2022). For *Typha,* herbivory occurred more in *T. latifolia*, resulting in higher biomass die-off, which most likely caused more respiration than in *T. angustifolia*.

The C-export term in *Typha* contributes to the net CO_2 balance with about 27-51 % (Table 3). This term is, however, not the
445 C from the total produced biomass, since dead biomass from the previous year was subtracted to make the balance right. Yields of 10-25 t dm ha^{-1} yr^{-1} can be possible (Geurts and Fritz, 2018), while our site showed 8 (*T. latifolia*) to 11 (*T. angustifolia*) t dm ha^{-1} yr^{-1}.

The yield term assumes that all harvested carbon is decomposed to CO_2 again. This is the case if biomass is burned or used as fodder (although C-emission can also be in the form of CH_4 in this case), but if biomass is used sustainably for long term
450 storage such as building material, this C-export can be neglected. However, to know the exact GHG effect of biomass storage, a life cycle assessment is needed to account for all other emission terms. De Jong et al., (2021) estimated that using *Typha* as insulation material, emissions from cultivating and processing *Typha* would be 9.7 t CO_2-ha^{-1} yr^{-1}, which almost compensates the biomass harvest in *T. latifolia*. They also conclude that the largest GHG gain is reducing the peat oxidation and not in the biomass use.

455 If considering the effect of topsoil removal as well on the carbon balance, things start to look quite differently. If all the carbon that is removed from the top 20 cm (15.8 kg m^{-2}) is not stored under anoxic conditions, an amount of 557 t CO_2 ha^{-1} will be released over the period needed to decompose that carbon. That is the same amount the reference site is emitting in 27 years.

Therefore, if topsoil removal is applied, one should consider the potentially large CO_2 emission associated with topsoil decomposition.

460

4.3 Biochemical interactions with paludicrops

Our results indicate that both *Typha* spp. effectively reduced nutrients (N+P) in the surface water and pore water, which is consistent with the results of Vroom et al. (2018). In the *Azolla* compartment N (as ammonium) and P accumulated in the pore water, but concentrations in the surface water were also low. The removal of ~20 cm of the topsoil, and with that a reduction
465 of approximately 65% of soil total-P, probably resulted in strong P-limiting conditions for *Azolla* (Temmink et al., 2018) and possibly also for both *Typha* spp. (Lorenzen et al., 2001).

Rewetting without topsoil removal probably has a positive effect on biomass production, especially for *Azolla*. Recent studies have shown, however, that this could have a strongly stimulate CH_4 emission (Harpenslager et al., 2015; Quadra et al., 2023). Our results indicate that smart crop-choices can, to an extent, mitigate these effects. The high phosphate mobilisation often
470 associated with rewetting of former agricultural drained peatland without topsoil removal could create the right conditions for *Azolla* cultivation, while also reducing CH_4 emissions compared to *Typha* cultivation. *Azolla* can be used as a temporary crop while the phosphorus mobilisation-rates after rewetting are high (Forni et al., 2001; Temmink et al., 2018) and the system adjusts to continuously waterlogged conditions. Once the phosphorus-flux to the overlying water is reduced other (rooting) paludicrops could be introduced.

475 In coastal areas salinity plays an important role in crop choice. *T. angustifolia* is more salt-tolerant than *T. latifolia*, with an upper limit for *T. latifolia* between 1.6-2.7 g l^{-1} (Anderson, 1977), which is lower than concentrations we observed, which may partly explain the inhibited growth. For *T. angustifolia* our measured concentrations were also higher than the upper limit of 7.2-8.8 g l^{-1} (Sinicrope et al., 1990).

Even though *T. angustifolia* showed lower CH_4 emissions and higher salt tolerance, there are also advantages to use *T. latifolia*
480 as a paludicrop. *T. latifolia* is considered to be better suitable for building materials due to the higher yield and more optimal diameter (Haldan et al., 2022). Thereby, *T. latifolia* can also better grow with lower water tables, which could significantly reduce CH_4 emissions if water table drops below surface (Haldan et al., 2022; Vroom et al., In prep.).

Conclusion

Our results show that all paludiculture crops reduce GHG emission compared to an intensively used drained fen grassland,
485 with highest reduction for *Typha angustifolia* and lowest for *Typha latifolia*. CH_4 emission in CO_2-eq is very variable per species but can be as high or higher than the CO_2 emission from drained peatland but is (partly) compensated by net CO_2 uptake.

Typha is a rooting plant, resulting in plant mediated gas transport from the sediment to the atmosphere and easily degradable carbon input into the sediment. This leads to higher total CH_4 emission compared to *Azolla*, but also to a lower contribution of ebullition to the total CH_4 flux.

Topsoil removal did not lead to low CH_4 emissions, especially not for *Typha latifolia*. What did change was nutrient availability with topsoil removal. Probably leading to limiting growth of all species, but most for *Azolla*.

In our case study *Azolla* and *T. angustifolia* seem to have a high potential for peatland rewetting to reduce the impact on climate change. A follow-up study without e.g. topsoil removal would be interesting to see if *Azolla* would be more productive and keeping CH_4 emissions low.

Data availability

All raw data can be provided by the corresponding authors upon request.

Author contribution

BvdR, AS and MvdB designed the experiment. TG, RV, JvH, JB and CvH carried the experiment out. TG and RV did most of the data preparation. MvdB and TG prepared the manuscript. MvdB did most of the writing, followed by TG and RV. All other authors contributed to editing the manuscript.

Competing interests

The contact author has declared that neither of the authors has any competing interests.

Acknowledgement

The measurements on the paludiculture site were part of the Peat Innovation Program initiated by the Association for Agricultural Nature and Landscape Management; Water, Land & Dijken (WLD) and the landscape conservation organisation Landschap Noord-Holland (LNH). The measurements on the reference site were part of the Dutch national research program NOBV funded by the Dutch ministry of Agriculture, Nature and Food Quality. RV and BvdR were supported by the NWO-TTW-project AZOPRO (Project no. 16294).

References

Abdalla, M., Hastings, A., Truu, J., Espenberg, M., Mander, Ü., and Smith, P.: Emissions of methane from northern peatlands: a review of management impacts and implications for future management options, Ecol. Evol., 6, 7080–7102, https://doi.org/10.1002/ece3.2469, 2016.

Abel, S. and Kallweit, T.: Potential Paludiculture Plants of the Holarctic., Greifswald Mire Centre, Greifswald, 2022.

Anderson, C. M.: attail decline at Farmington Bay Waterfowl Management Area, Gt. Basin Nat., 37, 1977.

Antonijević, D., Hoffmann, M., Prochnow, A., Krabbe, K., Weituschat, M., Couwenberg, J., Ehlert, S., Zak, D., and Augustin, J.: The unexpected long period of elevated CH4 emissions from an inundated fen meadow ended only with the occurrence of cattail (Typha latifolia), Glob. Change Biol., 29, 3678–3691, https://doi.org/10.1111/gcb.16713, 2023.

Arets, E., Lesschen, JP., Lerink, B., Schelhaas, M.-J., and Hendriks, C.: Information on LULUCF actions, The Netherlands Reporting in accordance to Article 10 of Decision No 529/2013/EU, Wageningen Environmental Research, 2020.

Armstrong, J., Armstrong, W., Armstrong, I. B., and Pittaway, G. R.: Senescence, and phytotoxin, insect, fungal and mechanical damage: factors reducing convective gas-flows in Phragmites australis, Aquat. Bot., 54, 211–226, https://doi.org/10.1016/0304-3770(96)82384-9, 1996.

Attermeyer, K., Flury, S., Jayakumar, R., Fiener, P., Steger, K., Arya, V., Wilken, F., Van Geldern, R., and Premke, K.: Invasive floating macrophytes reduce greenhouse gas emissions from a small tropical lake, Sci. Rep., 6, 20424, https://doi.org/10.1038/srep20424, 2016.

Bastviken, D., Treat, C. C., Pangala, S. R., Gauci, V., Enrich-Prast, A., Karlson, M., Gålfalk, M., Romano, M. B., and Sawakuchi, H. O.: The importance of plants for methane emission at the ecosystem scale, Aquat. Bot., 184, 103596, https://doi.org/10.1016/j.aquabot.2022.103596, 2023.

Bendix, M., Tornbjerg, T., and Brix, H.: Internal gas transport in Typha latifolia L. and Typha angustifolia L. 1. Humidity-induced pressurization and convective throughflow, Aquat. Bot., 49, 75–89, https://doi.org/10.1016/0304-3770(94)90030-2, 1994.

Bharati, K., Mohanty, S. R., Singh, D. P., Rao, V. R., and Adhya, T. K.: Influence of incorporation or dual cropping of Azolla on methane emission from a flooded alluvial soil planted to rice in eastern India, Agric. Ecosyst. Environ., 79, 73–83, https://doi.org/10.1016/S0167-8809(99)00148-6, 2000.

Bocchi, S. and Malgioglio, A.: Azolla-Anabaena as a Biofertilizer for Rice Paddy Fields in the Po Valley, a Temperate Rice Area in Northern Italy, Int. J. Agron., 2010, 1–5, https://doi.org/10.1155/2010/152158, 2010.

Bonn, A., Allott, T., Evans, M., Joosten, H., and Stoneman, R. (Eds.): Peatland Restoration and Ecosystem Services: Science, Policy and Practice, 1st ed., Cambridge University Press, https://doi.org/10.1017/CBO9781139177788, 2016.

540 Boonman, J., Hefting, M. M., van Huissteden, C. J. A., van den Berg, M., Van Huissteden, J. (Ko), Erkens, G., Melman, R., and van der Velde, Y.: Cutting peatland CO_2 emissions with water management practices, Biogeosciences, 19, 5707–5727, https://doi.org/10.5194/bg-19-5707-2022, 2022.

Boström, B., Andersen, J. M., Fleischer, S., and Jansson, M.: Exchange of Phosphorus Across the Sediment-Water Interface, in: Phosphorus in Freshwater Ecosystems, edited by: Persson, G. and Jansson, M., Springer Netherlands, Dordrecht, 229–244, 545 https://doi.org/10.1007/978-94-009-3109-1_14, 1988.

Brouwer, P., Nierop, K. G. J., Huijgen, W. J. J., and Schluepmann, H.: Aquatic weeds as novel protein sources: Alkaline extraction of tannin-rich Azolla, Biotechnol. Rep., 24, e00368, https://doi.org/10.1016/j.btre.2019.e00368, 2019.

Buzacott, A., van den Berg, M., Kruijt, B., and van der Velde, Y.: A Bayesian inference approach to determine experimental Typha plot greenhouse gas exchange measured with eddy covariance, Prep, In prep.

550 Clements, D.: Typha latifolia (broadleaf cattail), CABI Compend., CABI Compendium, 54297, https://doi.org/10.1079/cabicompendium.54297, 2022.

De Jong, M., Van Hal, O., Pijlman, J., Van Eekeren, N., and Junginger, M.: Paludiculture as paludifuture on Dutch peatlands: An environmental and economic analysis of Typha cultivation and insulation production, Sci. Total Environ., 792, 148161, https://doi.org/10.1016/j.scitotenv.2021.148161, 2021.

555 Desrosiers, K., DelSontro, T., and Del Giorgio, P. A.: Disproportionate Contribution of Vegetated Habitats to the CH_4 and CO_2 Budgets of a Boreal Lake, Ecosystems, 25, 1522–1541, https://doi.org/10.1007/s10021-021-00730-9, 2022.

Forni, C., Chen, J., Tancioni, L., and Grilli Caiola, M.: Evaluation of the fern Azolla for growth, nitrogen and phosphorus removal from wastewater, Water Res., 35, 1592–1598, https://doi.org/10.1016/S0043-1354(00)00396-1, 2001.

Franz, D., Koebsch, F., Larmanou, E., Augustin, J., and Sachs, T.: High net CO_2 and CH_4 release at a eutrophic shallow lake 560 on a formerly drained fen, Biogeosciences, 13, 3051–3070, https://doi.org/10.5194/bg-13-3051-2016, 2016.

Geurts, J. and Fritz, C.: Paludiculture pilots and experiments with focus on cattail and reed in the Netherlands, Radboud University, Nijmegen, Netherlands, 2018.

Gremmen, T., van de Riet, B., van den Berg, M., Vroom, R. J. E., Weideveld, S. T. J., Van Huissteden, J., Westendorp, P.-J., and Smolders, A. J. P.: Natte teelten en veeteelt bij een verhoogd (grond)waterpeil in de veenweiden: de effecten van 565 vernattingsmaatregelen op biogeochemie & broeikasgasemissies, B-WARE, Nijmegen, Netherlands, 2022.

Grünfeld, S. and Brix, H.: Methanogenesis and methane emissions: effects of water table, substrate type and presence of Phragmites australis, Aquat. Bot., 64, 63–75, https://doi.org/10.1016/S0304-3770(99)00010-8, 1999.

Günther, A., Barthelmes, A., Huth, V., Joosten, H., Jurasinski, G., Koebsch, F., and Couwenberg, J.: Prompt rewetting of drained peatlands reduces climate warming despite methane emissions, Nat. Commun., 11, 1644, https://doi.org/10.1038/s41467-020-15499-z, 2020.

Hahn, J., Köhler, S., Glatzel, S., and Jurasinski, G.: Methane Exchange in a Coastal Fen in the First Year after Flooding - A Systems Shift, PLOS ONE, 10, e0140657, https://doi.org/10.1371/journal.pone.0140657, 2015.

Hahn-Schöfl, M., Zak, D., Minke, M., Gelbrecht, J., Augustin, J., and Freibauer, A.: Organic sediment formed during inundation of a degraded fen grassland emits large fluxes of CH4 and CO2, Biogeosciences, 8, 1539–1550, https://doi.org/10.5194/bg-8-1539-2011, 2011.

Haldan, K., Köhn, N., Hornig, A., Wichmann, S., and Kreyling, J.: Typha for paludiculture—Suitable water table and nutrient conditions for potential biomass utilization explored in mesocosm gradient experiments, Ecol. Evol., 12, https://doi.org/10.1002/ece3.9191, 2022.

Harpenslager, S. F., Van Den Elzen, E., Kox, M. A. R., Smolders, A. J. P., Ettwig, K. F., and Lamers, L. P. M.: Rewetting former agricultural peatlands: Topsoil removal as a prerequisite to avoid strong nutrient and greenhouse gas emissions, Ecol. Eng., 84, 159–168, https://doi.org/10.1016/j.ecoleng.2015.08.002, 2015.

Hemes, K. S., Chamberlain, S. D., Eichelmann, E., Knox, S. H., and Baldocchi, D. D.: A Biogeochemical Compromise: The High Methane Cost of Sequestering Carbon in Restored Wetlands, Geophys. Res. Lett., 45, 6081–6091, https://doi.org/10.1029/2018GL077747, 2018.

Hoogland, T., Van Den Akker, J. J. H., and Brus, D. J.: Modeling the subsidence of peat soils in the Dutch coastal area, Geoderma, 171–172, 92–97, https://doi.org/10.1016/j.geoderma.2011.02.013, 2012.

Humpenöder, F., Karstens, K., Lotze-Campen, H., Leifeld, J., Menichetti, L., Barthelmes, A., and Popp, A.: Peatland protection and restoration are key for climate change mitigation, Environ. Res. Lett., 15, 104093, https://doi.org/10.1088/1748-9326/abae2a, 2020.

Intergovernmental Panel On Climate Change: Climate Change 2021 – The Physical Science Basis: Working Group I Contribution to the Sixth Assessment Report of the Intergovernmental Panel on Climate Change, 1st ed., Cambridge University Press, https://doi.org/10.1017/9781009157896, 2021.

Jespersen, D. N., K. Sorrell, B., and Brix, H.: Growth and root oxygen release by Typha latifolia and its effects on sediment methanogenesis, Aquat. Bot., 61, 165–180, https://doi.org/10.1016/S0304-3770(98)00071-0, 1998.

595   Joabsson, A. and Christensen, T. R.: Methane emissions from wetlands and their relationship with vascular plants: an Arctic example: METHANE EMISSION and VASCULAR PLANTS, Glob. Change Biol., 7, 919–932, https://doi.org/10.1046/j.1354-1013.2001.00044.x, 2001.

Kimani, S. M., Cheng, W., Kanno, T., Nguyen-Sy, T., Abe, R., Oo, A. Z., Tawaraya, K., and Sudo, S.: Azolla cover significantly decreased CH 4 but not N 2 O emissions from flooding rice paddy to atmosphere, Soil Sci. Plant Nutr., 64, 68–
600   76, https://doi.org/10.1080/00380768.2017.1399775, 2018.

Kosten, S., Piñeiro, M., De Goede, E., De Klein, J., Lamers, L. P. M., and Ettwig, K.: Fate of methane in aquatic systems dominated by free-floating plants, Water Res., 104, 200–207, https://doi.org/10.1016/j.watres.2016.07.054, 2016.

Leifeld, J. and Menichetti, L.: The underappreciated potential of peatlands in global climate change mitigation strategies, Nat. Commun., 9, 1071, https://doi.org/10.1038/s41467-018-03406-6, 2018.

605   Li, F.-W., Brouwer, P., Carretero-Paulet, L., Cheng, S., de Vries, J., Delaux, P.-M., Eily, A., Koppers, N., Kuo, L.-Y., Li, Z., Simenc, M., Small, I., Wafula, E., Angarita, S., Barker, M. S., Bräutigam, A., dePamphilis, C., Gould, S., Hosmani, P. S., Huang, Y.-M., Huettel, B., Kato, Y., Liu, X., Maere, S., McDowell, R., Mueller, L. A., Nierop, K. G. J., Rensing, S. A., Robison, T., Rothfels, C. J., Sigel, E. M., Song, Y., Timilsena, P. R., Van de Peer, Y., Wang, H., Wilhelmsson, P. K. I., Wolf, P. G., Xu, X., Der, J. P., Schluepmann, H., Wong, G. K.-S., and Pryer, K. M.: Fern genomes elucidate land plant evolution
610   and cyanobacterial symbioses, Nat. Plants, 4, 460–472, https://doi.org/10.1038/s41477-018-0188-8, 2018.

Liu, J., Xu, H., Jiang, Y., Zhang, K., Hu, Y., and Zeng, Z.: Methane Emissions and Microbial Communities as Influenced by Dual Cropping of Azolla along with Early Rice, Sci. Rep., 7, 40635, https://doi.org/10.1038/srep40635, 2017.

Lorenzen, B., Brix, H., Mendelssohn, I. A., McKee, K. L., and Miao, S. L.: Growth, biomass allocation and nutrient use efficiency in Cladium jamaicense and Typha domingensis as affected by phosphorus and oxygen availability, Aquat. Bot., 70,
615   117–133, https://doi.org/10.1016/S0304-3770(01)00155-3, 2001.

Maltais-Landry, G., Maranger, R., Brisson, J., and Chazarenc, F.: Greenhouse gas production and efficiency of planted and artificially aerated constructed wetlands, Environ. Pollut., 157, 748–754, https://doi.org/10.1016/j.envpol.2008.11.019, 2009.

Martens, M., Karlsson, N. P. E., Ehde, P. M., Mattsson, M., and Weisner, S. E. B.: The greenhouse gas emission effects of rewetting drained peatlands and growing wetland plants for biogas fuel production, J. Environ. Manage., 277, 111391,
620   https://doi.org/10.1016/j.jenvman.2020.111391, 2021.

Matsui Inoue, T. and Tsuchiya, T.: Interspecific differences in radial oxygen loss from the roots of three Typha species, Limnology, 9, 207–211, https://doi.org/10.1007/s10201-008-0253-5, 2008.

McInerney, E. and Helton, A. M.: The Effects of Soil Moisture and Emergent Herbaceous Vegetation on Carbon Emissions from Constructed Wetlands, Wetlands, 36, 275–284, https://doi.org/10.1007/s13157-016-0736-9, 2016.

625 McMillan, C.: Salt tolerance within a Typha population, Am. J. Bot., 46, 521–526, https://doi.org/10.1002/j.1537-2197.1959.tb07044.x, 1959.

Minick, K. J., Mitra, B., Noormets, A., and King, J. S.: Saltwater reduces potential CO2 and CH4 production in peat soils from a coastal freshwater forested wetland, Biogeosciences, 16, 4671–4686, https://doi.org/10.5194/bg-16-4671-2019, 2019.

Minke, M., Augustin, J., Burlo, A., Yarmashuk, T., Chuvashova, H., Thiele, A., Freibauer, A., Tikhonov, V., and Hoffmann,
630 M.: Water level, vegetation composition, and plant productivity explain greenhouse gas fluxes in temperate cutover fens after inundation, Biogeosciences, 13, 3945–3970, https://doi.org/10.5194/bg-13-3945-2016, 2016.

Miranda, A. F., Biswas, B., Ramkumar, N., Singh, R., Kumar, J., James, A., Roddick, F., Lal, B., Subudhi, S., Bhaskar, T., and Mouradov, A.: Aquatic plant Azolla as the universal feedstock for biofuel production, Biotechnol. Biofuels, 9, 221, https://doi.org/10.1186/s13068-016-0628-5, 2016.

635 Murphy, K.: Typha angustifolia (lesser bulrush), https://doi.org/10.1079/cabicompendium.54294, 2022.

Pazourek, J.: The volumes of anatomical components in leaves of Typha angustifolia L. and Typha latifolia L., Biol. Plant., 19, 129–135, 1977.

Pijlman, J., Guerts, J., Vroom, R., Bestman, M., Fritz, C., and van Eekeren, N.: The effects of harvest date and frequency on the yield, nutritional value and mineral content of the paludiculture crop cattail (Typha latifolia L.) in the first year after
640 planting, Mires Peat, 1–19, https://doi.org/10.19189/MaP.2017.OMB.325, 2019.

Pinero-Rodríguez, M. J., Fernández-Zamudio, R., Arribas, R., Gomez-Mestre, I., and Díaz-Paniagua, C.: The invasive aquatic fern Azolla filiculoides negatively impacts water quality, aquatic vegetation and amphibian larvae in Mediterranean environments, Biol. Invasions, 23, 755–769, https://doi.org/10.1007/s10530-020-02402-6, 2021.

Quadra, G. R., Boonman, C. C. F., Vroom, R. J. E., Temmink, R. J. M., Smolders, A. J. P., Geurts, J. J. M., Aben, R. C. H.,
645 Weideveld, S. T. J., and Fritz, C.: Removing 10 cm of degraded peat mitigates unwanted effects of peatland rewetting: a mesocosm study, Biogeochemistry, 163, 65–84, https://doi.org/10.1007/s10533-022-01007-6, 2023.

Rey-Sanchez, A. C., Morin, T. H., Stefanik, K. C., Wrighton, K., and Bohrer, G.: Determining total emissions and environmental drivers of methane flux in a Lake Erie estuarine marsh, Ecol. Eng., 114, 7–15, https://doi.org/10.1016/j.ecoleng.2017.06.042, 2018.

650 Sebacher, D. I., Harriss, R. C., and Bartlett, K. B.: Methane Emissions to the Atmosphere Through Aquatic Plants, J. Environ. Qual., 14, 40–46, https://doi.org/10.2134/jeq1985.00472425001400010008x, 1985.

Sinicrope, T. L., Hine, P. G., Warren, R. S., and Niering, W. A.: Restoration of an Impounded Salt Marsh in New England, Estuaries, 13, 25, https://doi.org/10.2307/1351429, 1990.

Strachan, I. B., Nugent, K. A., Crombie, S., and Bonneville, M.-C.: Carbon dioxide and methane exchange at a cool-temperate freshwater marsh, Environ. Res. Lett., 10, 065006, https://doi.org/10.1088/1748-9326/10/6/065006, 2015.

Temmink, R. J. M., Harpenslager, S. F., Smolders, A. J. P., Van Dijk, G., Peters, R. C. J. H., Lamers, L. P. M., and Van Kempen, M. M. L.: Azolla along a phosphorus gradient: biphasic growth response linked to diazotroph traits and phosphorus-induced iron chlorosis, Sci. Rep., 8, 4451, https://doi.org/10.1038/s41598-018-22760-5, 2018.

Van den Berg, M., van den Elzen, E., Ingwersen, J., Kosten, S., Lamers, L. P. M., and Streck, T.: Contribution of plant-induced pressurized flow to CH4 emission from a Phragmites fen, Sci. Rep., 10, 12304, https://doi.org/10.1038/s41598-020-69034-7, 2020.

Van den Born, G. J., Kragt, F., Henkens, D., Rijken, van Bemmel, B., and van der Sluis, S.: Dalende bodems, stijgende kosten, PBL, Den Haag, 2016.

Van der Gon, H. A. C. D. and Neue, H.-U.: Methane emission from a wetland rice field as affected by salinity, Plant Soil, 170, 307–313, https://doi.org/10.1007/BF00010483, 1995.

Van der Nat, F. W. A., Middelburg, J. J., van Meteren, D., and Wielemakers, A.: Diel methane emission patterns from Scirpus lacustris and Phragmites australis, Biogeochemistry, 41, 1–22, 1998.

Van Kempen, M. M.: Azolla on top of the world: an ecophysiological study of floating fairy moss and its potential role in ecosystem services related to climate change, PhD Thesis, SI:[Sn], 2013.

Vroom, R. J. E., Xie, F., Geurts, J. J. M., Chojnowska, A., Smolders, A. J. P., Lamers, L. P. M., and Fritz, C.: Typha latifolia paludiculture effectively improves water quality and reduces greenhouse gas emissions in rewetted peatlands, Ecol. Eng., 124, 88–98, https://doi.org/10.1016/j.ecoleng.2018.09.008, 2018.

Vroom, R. J. E., van den Berg, M., Pangala, S. R., van der Scheer, O. E., and Sorrell, B. K.: Physiological processes affecting methane transport by wetland vegetation – A review, Aquat. Bot., 182, 103547, https://doi.org/10.1016/j.aquabot.2022.103547, 2022.

Vroom, R. J. E., Gremmen, T., van Huissteden, J., Smolders, A. J. P., van de Riet, B., Kosten, S., Fritz, C., and van den Berg, M.: Chimneys and blankets : species-dependent methane emissions in a rewetted Dutch peatland, In prep.

Wagner, G. M.: Azolla: A review of its biology and utilization, Bot. Rev., 63, 1–26, https://doi.org/10.1007/BF02857915, 1997.

680   White, S. D. and Ganf, G. G.: Flow characteristics and internal pressure profiles in leaves of the Typha domingensis, Aquat. Bot., 67, 263–273, https://doi.org/10.1016/S0304-3770(00)00100-5, 2000.

Wichtmann, W. and Joosten, H.: Paludiculture: Peat formation and renewable resources from rewetted peatlands, IMCG Newsletter, 3, 2007.

Xu, H., Zhu, B., Liu, J., Li, D., Yang, Y., Zhang, K., Jiang, Y., Hu, Y., and Zeng, Z.: Azolla planting reduces methane emission
685   and nitrogen fertilizer application in double rice cropping system in southern China, Agron. Sustain. Dev., 37, 29, https://doi.org/10.1007/s13593-017-0440-z, 2017.

Yavitt, J. B. and Knapp, A. K.: Aspects of methane flow from sediment through emergent cattail (Typha latifolia) plants, New Phytol., 139, 495–503, https://doi.org/10.1046/j.1469-8137.1998.00210.x, 1998.

690

Appendix A Biogeochemical data

Table A1 Surface water chemistry of pH, alkalinity (Alk), electric conductivity (EC), total inorganic carbon (TIC), nitrate (NO₃⁻), ammonium (NH₄⁺), phosphate (PO₄³⁻), chloride (Cl), total iron (TFe), potassium (K), magnesium (Mg), sodium (Na), total phosphorus (TP), total sulphur (TS), total organic carbon (TOC) and total organic nitrogen (TON) measured in the plots of the three different paludicrops. Measurements were taken over the whole season (n = 9-12) and averaged. The numbers between the brackets denote the minimum and maximum measured.

Variable	Unit	Inlet water	*Azolla*	*T. angustifolia*	*T. latifolia*
pH	n.a.	7.8 [7.3, 8.4]	7.6[7.0, 8.4]	7.4 [7.0, 7.7]	7.7 [7.1, 8.6]
Alk	meq l−1	5.2 [2.1, 7.2]	4.9 [1.8, 6.8]	4.4 [1.8, 6.5]	4.1 [1.8, 5.8]
EC	mS cm−1	4.8 [1.4, 7.3]	4.4 [1.3, 6.7]	4.0 [1.3, 6.2]	3.6 [1.2, 6.3]
TIC	mmol l-1	5.0 [1.7, 7.6]	5.0 [1.6, 7.3]	4.6 [1.4, 6.3]	4.1 [1.4, 6.0]
NO₃⁻	µmol l−1	9.4 [0.65, 58]	4.0 [0.55, 19]	1.6 [0.50, 5.1]	1.1 [0.28, 3.0]
NH₄⁺	µmol l−1	18 [3.1, 110]	15 [1.7, 82]	5.2 [1.9, 14]	4.9 [1.9, 15]
PO₄³⁻	µmol l−1	3.7 [0.97, 9.2]	2.4 [0.75, 5.2]	1.0 [0.17, 2.1]	1.2 [0.16, 2.4]
Cl⁻	mmol l-1	41 [9.2, 60]	39 [8.2, 60]	36 [8.3, 61]	33 [8.2, 62]
TFe	µmol l−1	39 [30, 72]	32 [17, 49]	33 [10, 66]	55 [18, 160]
K	mmol l-1	1.3 [0.20, 2.8]	1.2 [0.18, 2.7]	1.1 [0.18, 2.0]	1.0 [0.18, 2.0]
Mg	mmol l-1	3.5 [0.87, 5.1]	3.2 [0.73, 4.7]	2.8 [0.70, 4.3]	2.6 [0.70, 4.3]
Na	mmol l-1	40 [7.9, 71]	37 [7.1, 66]	33 [7.1, 53]	30 [6.9, 54]
TP	µmol l−1	9.9 [3.6, 19]	7.4 [3.0, 14]	3.6 [2.5, 5.3]	4.4 [2.2, 6.7]
TS	mmol l-1	1.1 [0.50, 1.4]	0.78 [0.39, 1.3]	0.46 [0.22, 0.89]	0.25 [0.13, 0.43
TOC	mmol l-1	5.3 [3.3, 8.6]	5.1 [3.7, 8.1]	4.8 [3.6, 6.7]	5.3 [3.4, 6.8]
TON	mmol l-1	0.28 [0.20, 0.42]	0.26 [0.19, 0.36]	0.21 [0.17, 0.27]	0.22 [0.17, 0.29]

700 **Table A2 Pore water chemistry of pH, electric conductivity (EC), total inorganic carbon (TIC), nitrate (NO₃⁻), ammonium (NH₄⁺), chloride (Cl), total iron (TFe), potassium (K), magnesium (Mg), sodium (Na), total phosphorus (TP) and total sulphur (TS) , hydrogen sulphide (H₂S), dissolved organic carbon (DOC) and dissolved organic nitrogen (DON) measured in the plots of the three different paludicrops. Measurements were taken over the whole season (n = 8-10) and averaged. The numbers between the brackets denote the minimum and maximum measured.**

705

Variable	Unit	*Azolla*	*T. angustifolia*	*T. latifolia*
pH	n.a	6.4 [6.2, 6.7]	4.8 [4.7, 5.0]	6.5 [6.3, 6.7]
EC	mS cm⁻1	4.6 [3.5, 6.5]	5.6 [4.0, 7.3]	4.7 [3.1, 7.0]
TIC	mmol l-1	8.2 [6.4, 11]	4.4 [3.1, 5.8]	7.9 [5.8, 10]
NO₃-	μmol l−1	3.1 [0.9, 8.6]	1.8 [0.4, 4.7]	1.1 [0.3 2.7]
NH₄⁺	μmol l−1	339 [129, 649]	11 [1, 28]	6.4 [2.9, 14]
Cl⁻	mmol l-1	40 [25, 57]	52 [32, 69]	41 [24, 63]
TFe	μmol l−1	1402 [114, 3275]	411 [298, 514]	62 [37, 91]
K	mmol l-1	1.0 [0.28, 1.9]	1.0 [0.67, 1.4]	0.95 [0.56, 1.3]
Mg	mmol l-1	3.2 [2.2, 4.6]	2.3 [1.3, 3.3]	3.4 [1.9, 5.5]
Na	mmol l-1	38 [25, 55]	48 [32, 64]	38 [23, 59]
TP	μmol l−1	29 [9.3, 56]	2.4 [1.1, 4.4]	1.6 [1.0, 2.9]
TS	mmol l-1	0.56 [0.18, 1.3]	0.27 [0.20, 0.45]	0.24 [0.11, 0.72]
H₂S	μmol l−1	0.024 [0.004, 0.072]	0.052 [0.007, 0.14]	0.023 [0.005, 0.052]
DOC	mmol l-1	24 [7.2, 59]	8.3 [6.3, 11]	5.2 [4.5, 5.8]
DON	mmol l-1	1.5 [0.61, 2.8]	0.34 [0.24, 0.43]	0.22 [0.19, 0.25]